

FUNERAL MASK IVC 11595 – CU/AG, WITH SURFACE ENRICHMENT (AG) – UNKNOWN – PERU

Artefact name Funeral mask Ivc 11595

Authors Christian. Degrygn (HE-Arc CR, Neuchâtel, Neuchâtel, Switzerland) & Naima. Gutknecht (HE-Arc CR, Neuchâtel, Neuchâtel, Switzerland) & Valentin. Boissonnas (HE-Arc CR, Neuchâtel, Neuchâtel, Switzerland)

Url /artefacts/1555/

∨ The object



Fig. 1: Funeral mask, front and back face to the left and right respectively,

Credit HE-Arc CR, N.Gutknecht.

∨ Description and visual observation

Description of the artefact	Peruvian funeral mask (Fig. 1). There are remains of red pigment and of a mineralised textile on both sides of the object. It is heavily corroded in green and red corrosion layers. It is deformed and broken. Dimensions: Length = 180mm; Width = 170mm; Height = 20 mm; WT = 158,6g.
Type of artefact	Funeral mask
Origin	Funeral mask, Peru
Recovering date	Date of excavation unknown, acquisition in 1967
Chronology category	Unknown
chronology tpq	<input type="text"/> ---- ∨
chronology taq	<input type="text" value="1500"/> A.D. ∨
Chronology comment	Tpq: unknown.
Burial conditions / environment	Unknown
Artefact location	Museum der Kulturen, Basel
Owner	Museum der Kulturen, Basel
Inv. number	Ivc 11595
Recorded conservation data	N/A

Complementary information

None.

∨ Study area(s)

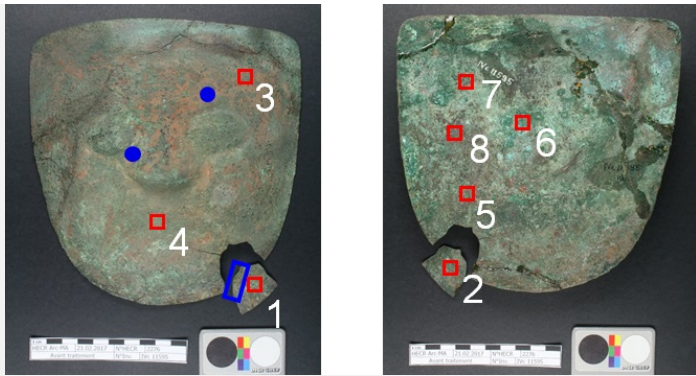


Fig. 2: Front (left) and back (right) faces showing the location of XRF analyses (red squares), sampling areas for SEM-EDS (blue points) and sampling area for examination on cross-section (blue rectangle),

Credit HE-Arc CR, N.Gutknecht.

Binocular observation and representation of the corrosion structure

The schematic representation below gives an overview of the corrosion layers encountered on the object from visual macroscopic observation. The first stratigraphy (Fig. 3a) is for the front, while the second (Fig. 3b) represents the back.

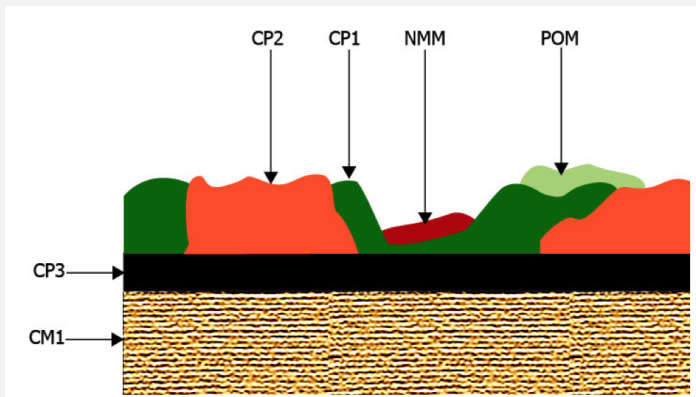


Fig. 3a: Stratigraphic representation of the front face of the funeral mask by visual macroscopic observation,

POM: Textile remains, **NMM:** Pigments, **CP1:** Green corrosion products, **CP2:** Red corrosion products, **CP4:** Black corrosion products, **CM1:** Remaining metal

Credit HE-Arc CR, N.Gutknecht.

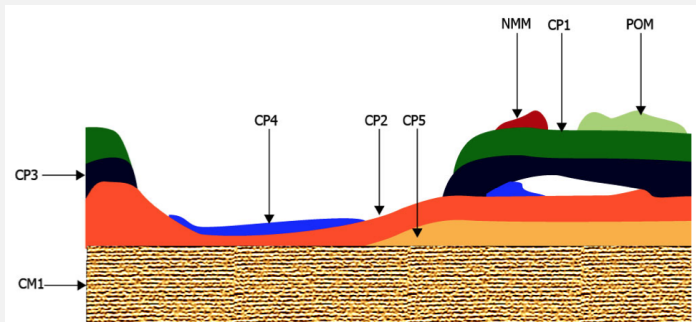


Fig. 3b: Stratigraphic representation of the back face of the funeral mask by visual macroscopic observation,

POM: Textile remains, **NMM:** Pigments, **CP1:** Green corrosion products, **CP2:** Red/orange corrosion products, **CP3:** Black corrosion product, **CP4:** blue corrosion product, **CP5:** Orange corrosion, **CM1:** Remaining metal

Credit HE-Arc CR, N.Gutknecht.

MiCorr stratigraphy(ies) – Bi

Sample(s)

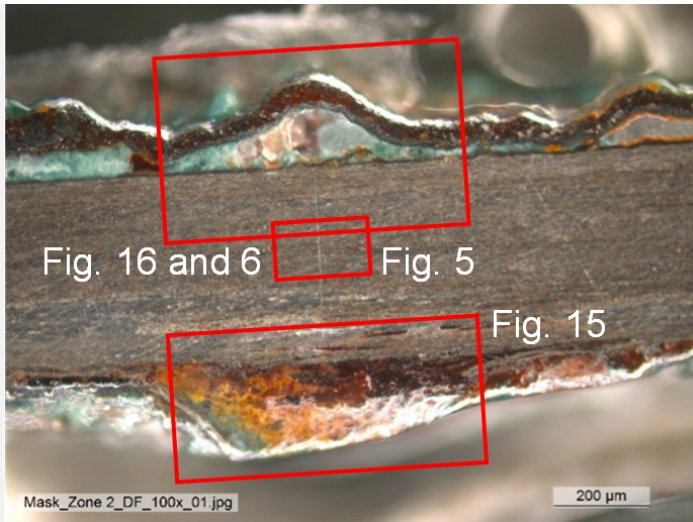


Fig. 4: Micrograph of the cross-section of the sample temporarily taken from the detached fragment of Fig. 2 showing the locations of Figs. 15 (corresponding to the front of the funeral mask), 16 (back of the funeral mask), 5 and 6,

Description of sample

A polished section was made from an already detached fragment that was temporarily embedded in resin (Fig. 2). On Fig. 4 the upper part of the sample corresponds to the back face of the funeral mask while the lower part corresponds to its front face. Both sides have developed subsequent layers of corrosion. In areas, these have buckled and become detached.

Alloy

Cu/Ag, with surface enrichment (Ag)

Technology

Hammered and annealed, surface depletion

Lab number of sample

None

Sample location

None

Responsible institution

Museum der Kulturen, Basel

Date and aim of sampling

2017, metallography and chemical analyses

Complementary information

None.

Analyses and results

Analyses performed:

XRF with portable X-ray fluorescence spectrometer (NITON XL3t 950 Air GOLDD+ analyser, Thermo Fischer®, SEM/EDS (with an acceleration voltage of 20 kV) and Raman spectroscopy.

Non invasive analysis

The XRF analysis is a surface analysis that was done without any removal of the copper corrosion products. It seems that the metal is a copper-silver alloy.

Metal

The SEM/EDS analysis of the core metal shows that there are Cu-rich phases alternating with Ag-rich phases. There are inclusions of Pb and As (Fig. 5). The surface of the metal has been decuprified (Fig. 6) according to the tumbaga making process (Scott 2000 and McEwan 2000). This pre-Columbian repeatedly hammered and annealed the metal, which would create a copper oxide scale on the surface. The latter was then dissolved in acidic plant juices (Scott 2000). This process was repeated until the surface was enriched with silver, giving it the appearance of a silver artefact.

It is impossible to know the original alloy composition, as the proportions have changed through corrosion and migration of elements. Nevertheless, the inner metal is reddish, which could indicate a 30% silver content for 70% copper. For this artefact, the silver-rich surface has been further enriched by the migration of copper ions that have formed the thick corrosion crust on top of the original surface.

A layer of mercury can be seen with EDS (Figs. 6 and 7). Mercury was not used by the pre-Columbians in metallic form (Scott 2000 and McEwan 2000) but was common as a pigment in form of mercury sulfide (cinnabar).

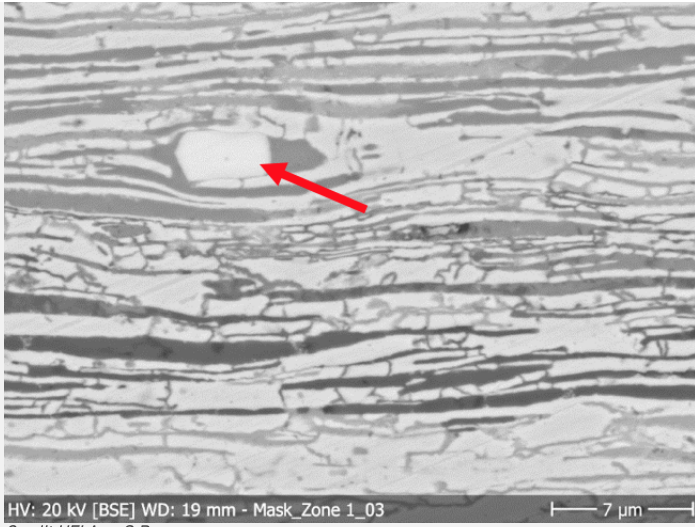


Fig. 5: SEM image (BSE-mode) of the metal sample from Fig. 4 (detail), the elongated grains are the result of repeated hammering. Absence of strain lines indicates that the metal is annealed. The darker areas are Cu-rich phases and the lighter areas are Ag-rich phases. The arrow shows an As- and Pb inclusion,

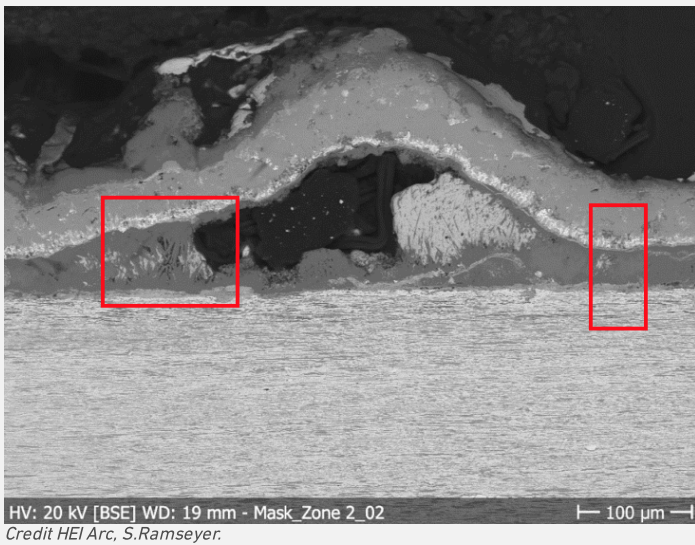


Fig. 6: SEM image (BSE-mode) of the metal sample from Fig. 4 with detail (Fig. 7) indicated by the left red rectangle. The selected area for elemental chemical distribution (Fig. 8) is marked by the right red rectangle,

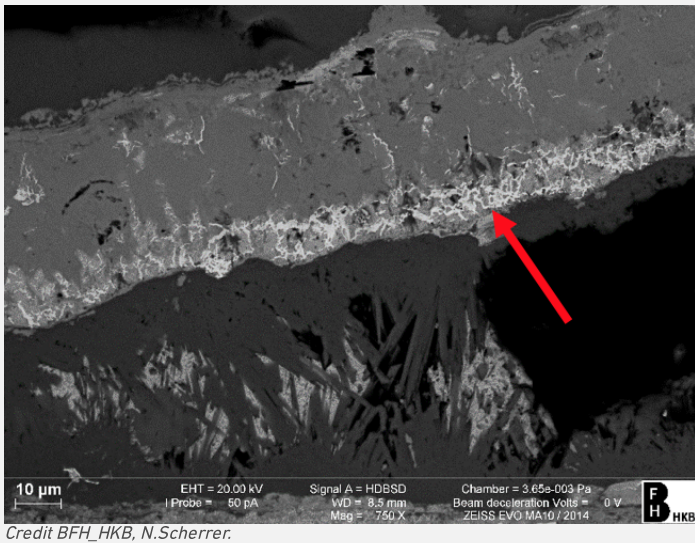


Fig. 7: SEM image of a partially refilled structural void with a silver-, copper- and mercury-rich layer (red arrow),

Microstructure	Unknown
First metal element	Cu
Other metal elements	As, Ag, Pb

Complementary information

None.

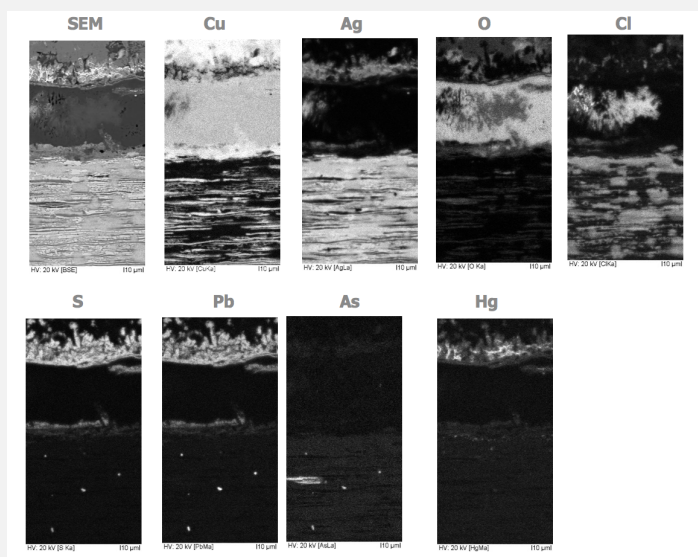
The remaining metal shows a preferential corrosion of copper and the presence of chlorides throughout the entire corroded metal, most likely in the form of Cu and Ag corrosion products (Fig. 8, Table 1). There is a preferential corrosion of copper that has fragilized the structure of the sheet metal.

The silver enriched surface is entirely covered with copper corrosion products. The outer green layer (CP1) is a copper carbonate (Fig. 11, Table 1), while the red layers (CP2 in Fig. 15 ; CP4 and CP5 in Fig. 16) are consisting of a copper oxide, most likely cuprite (Fig. 9). Below the cuprite and above the silver enriched surface on the front face a thin black layer is present (appears grey under polarized light). SEM-EDS analysis shows that in that stratum the mercury of the pigment (Fig. 14) has been transformed into a mercury-silver compound (Figs. 7 and 10) which according to Raman spectrometry (Fig. 14) is not cinnabar anymore. In areas this silver- and mercury-rich surface has been pulled off by raising the corrosion layers, leaving structural voids that were subsequently filled by secondary corrosion products, most likely copper carbonates (Figs. 6 and 7).

The silver sulphide (HgS, cinnabar, Fig. 13), present as a red pigment on the silver surface, could have been reduced through an electrochemical process in the presence of chlorides (Keune 2005). The released sulfur recombined with the silver to form black silver sulphide. Above that layer a porous mercury- and silver rich stratum has formed (see Hg & Ag on cartography Fig. 8). It remains unclear if the limitos is located in the silver enriched surface or within this silver-mercury compound (Fig. 7).

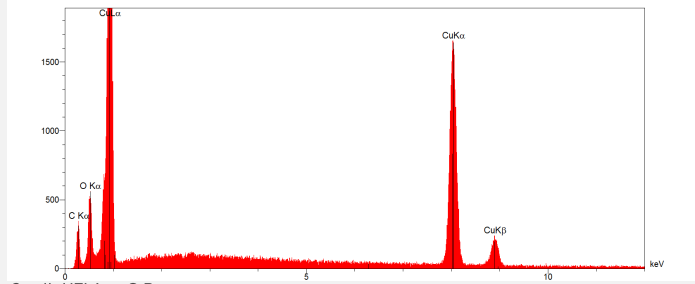
Elements	Cu	Ag	O	Cl	Hg	S	As	Pb	Interpretation
Red layer (CP2, front & CP4-CP5, back)	+++		+						Copper oxide
Grey layer (CP3, front & CP2, back)		+++			+++	++			Pigment (HgS) and silver
Green layer (CP1)	+++		+	++					Copper carbonate
Black layer	+	++				++			Silver and copper sulfides
Nodules in the metal		+++		+++					Silver chlorides
Metal phases 1	+	+++							Silver-rich phases
Metal phases 2	+++	++	+	+					Copper-rich phase
Inclusion in metal			+				++	+++	AsPb impurities

Table 1: Chemical composition of the corrosion crust from Fig. 4. Method of analysis: SEM-EDS, Lab of Electronic Microscopy and Microanalysis, IMA (Néode), HEI Arc (+++ : high concentration, ++ medium concentration, + low concentration), credit HEI Arc, S.Ramseyer.



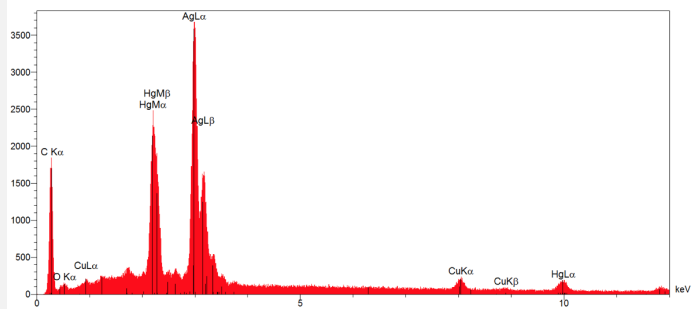
Credit HEI Arc_S.Ramseyer

Fig. 8: SEM image (BSE-mode) and elemental chemical distribution of the selected area on Fig. 6. Method of examination: SEM/EDS,

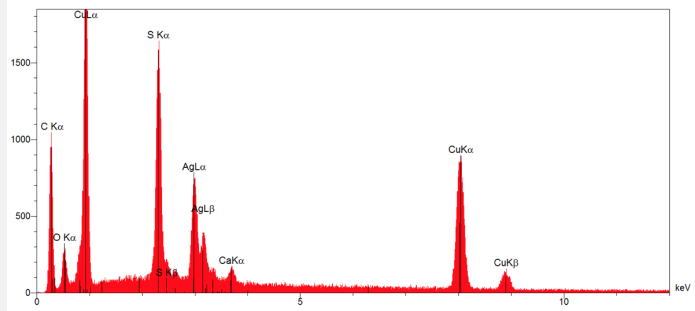


Credit HEI Arc, S.Ramseyer.

Fig. 9: EDS analysis of the red corrosion layer (Fig. 4). Method of analysis: SEM-EDS, Lab of Electronic Microscopy and Microanalysis, IMA (Néode), HEI Arc,

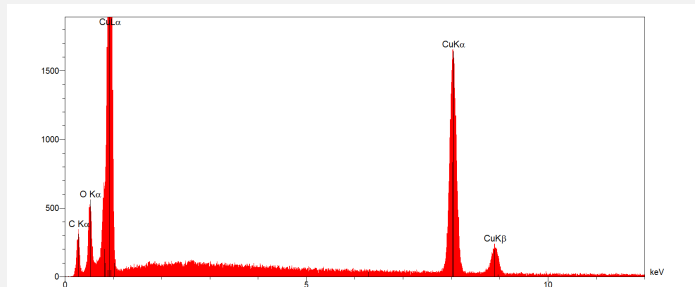


Figs. 10: EDS analysis of the layer that appears light grey under polarized light, situated below the red layer (Fig. 4). Method of analysis: SEM-EDS, Lab of Electronic Microscopy and Microanalysis, IMA (Néode), HEI Arc,



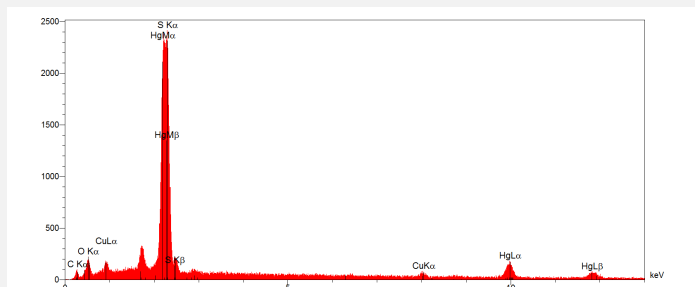
Credit HEI Arc, S.Ramseyer.

Fig. 11: EDS analysis of the green corrosion layer that has filled the structural void (Fig. 4). Method of analysis: SEM-EDS, Lab of Electronic Microscopy and Microanalysis, IMA (Néode), HEI Arc,

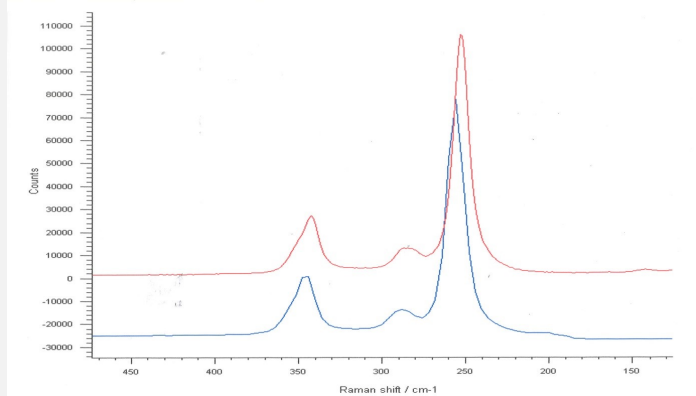


Credit HEI Arc, S.Ramseyer.

Fig. 12: EDS analysis of the red surface pigment from a surface sample. Method of analysis: SEM-EDS, Lab of Electronic Microscopy and Microanalysis, IMA (Néode), HEI Arc,

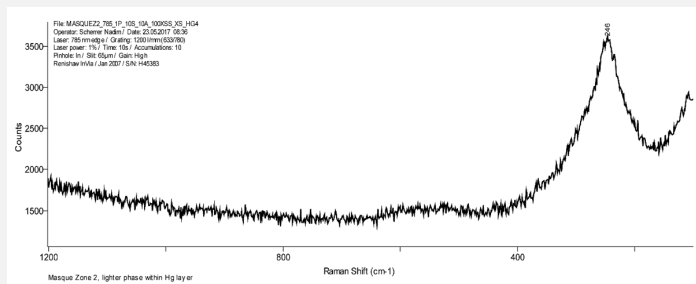


Credit HEI Arc, S.Ramseyer.



Credit HEI Arc, N.Scherrer.

Fig. 13: Raman analysis of the red pigment on the surface (red line) and the references for cinnabar (blue line). Method of analysis: Raman spectroscopy, HKB,



Credit HEI Arc, N.Scherrer.

Fig. 14: Raman analysis of the mercury compounds from the cross section. Method of analysis: Raman spectroscopy, HKB,

Corrosion form Uniform - selective

Corrosion type Unknown

Complementary information

None.

✄ MiCorr stratigraphy(ies) – CS

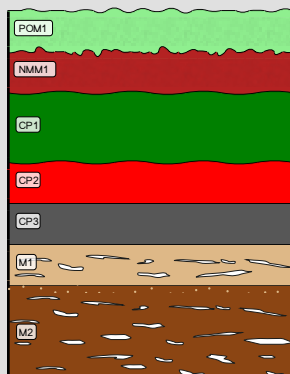


Fig. 15: Stratigraphic representation of the cross-section (dark field) from Figs. 3a or 4 (front of the object) using the MiCorr application. The characteristics of the strata are only accessible by clicking on the drawing that redirects you to the search tool by stratigraphy representation, Credit HE-Arc CR, N. Gutknecht.

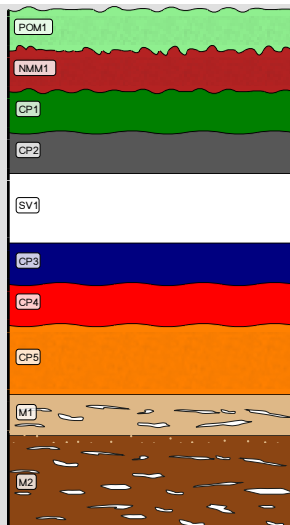


Fig. 16: Stratigraphic representation of the cross-section (dark field) from Figs. 3b and 4 (back of the object) using the MiCorr application. CP2 is CP3 while CP3 is CP4 and CP4 is CP2 in Fig. 3b. The characteristics of the strata are only accessible by clicking on the drawing that redirects you to the search tool by stratigraphy representation, Credit HE-Arc CR, N. Gutknecht.

✧ Synthesis of the binocular / cross-section examination of the corrosion structure

The schematic representation of corrosion layers of Fig. 3 integrating additional information based on the analyses carried out is given in Fig. 17.

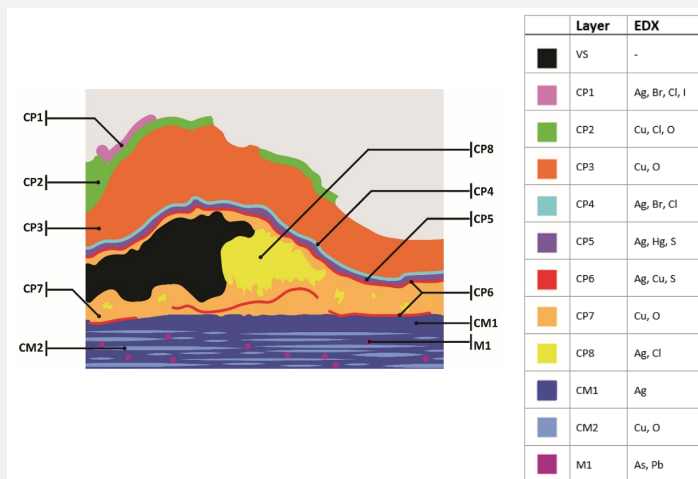


Fig. 17: Improved stratigraphic representation of the funeral mask (Fig. 3) based on the results from the SEM-EDS analyses,

Credit HE-Arc CR, N. Gutknecht

✧ Conclusion

The artefact is a repeatedly hammered, annealed and pickled Cu-Ag tumbaga. The cuprite and hydroxycarbonate layers and the presence of chlorides are typical for the corrosion of tumbaga alloys in an archaeological context. Cinnabar has been identified as pigment applied to the surface before burial. Over the centuries, it was partially incorporated into the growing copper corrosion layers.

Close to the enriched silver surface and below the cuprite layer a silver- and mercury-rich stratum has formed. Only one publication mentions the reaction of cinnabar with a gold-enriched tumbaga surface but does not go into details about the possible mechanism involved (Masuda 1997).

The presence of a silver-sulphur compound below this silver-mercury stratum could indicate that the cinnabar was reduced by electrochemical processes to mercury, releasing sulphur that reacted with the silver enriched surface. The mercury itself formed a silver-mercury layer above the latter. More research is needed to fully comprehend this phenomenon.

✧ References

References on object and sample

Reference objects

1. Keune, K. (2005) «Analytical Imaging Studies Clarifying the Process of the Darkening of Vermilion in Paintings». Analytical Chemistry, n° 77, 4742-4750.
2. Scott, D. (2000) A review of gilding techniques in ancient South America. In: T. Drayman-Weisser (ed.) Gilded Metals: History, Technology and Conservation. London, Archetype Publications, 203-222.
3. McEwan, C (ed.) (2000) Precolumbian Gold – Technology, style and Iconography. British Museum, London.
4. Masuda, S. (ed.) (1997) Sicàn - ein Fürstengrab in Alt-Peru: Eine Ausstellung in Zusammenarbeit mit dem peruanischen Kulturministerium. Museum Rietberg, Zurich.

